

## Original Research Article

# Anti-inflammatory effects of bitongling granules are mediated through the suppression of miR-21/p38 MAPK/TLR4/NF- $\kappa$ B signaling in H9C2 rat cardiac cells exposed to lipopolysaccharides

Yun-Xiang Cao<sup>1</sup>, Dan Huang<sup>1</sup>, Rui Lin<sup>2</sup>, Rui-Kai Zong<sup>1</sup>, Chuan-Bing Huang<sup>1</sup>, Yue Wang<sup>3\*</sup>, Jian Liu<sup>1\*</sup>

<sup>1</sup>Department of Rheumatology, The First Affiliated Hospital of Anhui University of Chinese Medicine, 117 Meishan Rd, Hefei 230031, <sup>2</sup>The Nanjing University of Chinese Medicine, 138 Xianlin Road, Nanjing 210046, China, <sup>3</sup>The Affiliated Hospital of Nanjing University of Chinese Medicine, 155 hanzhong road, Nanjing 210000.

\*For correspondence: **Email:** caoyx190522@hotmail.com

Sent for review: 26 October 2020

Revised accepted: 11 February 2022

### Abstract

**Purpose:** To assess the protective effects of bitongling granules on H9C2 cells exposed to lipopolysaccharides (LPS) in the management of rheumatoid arthritis (RA)-induced myocardial inflammation.

**Methods:** The effects of bitongling granule (BTLG) drug-containing serum were assessed in myocarditis models established in rat cardiac cells. MicroRNA-21 (miR-21) levels were evaluated by qRT-PCR while MTT assays were performed to assess cell viability. ELISA assay was used to evaluate tumor necrosis factor  $\alpha$  (TNF- $\alpha$ ), interleukin 17 (IL-17) and interleukin 6 (IL-6) levels in cell culture supernatants. Apoptosis was determined by flow cytometry (FCM). Quantitative mitogen-activated protein kinase (MAPK)/p38, toll-like receptor 4 (TLR4) and nuclear factor kappa B (NF- $\kappa$ B)/p65 levels were evaluated by western blot and immunofluorescence

**Results:** BTLG increased cardiac cell activity and exhibited anti-inflammatory effect. It also inhibited LPS-induced H9C2 apoptosis and suppressed p65 NF- $\kappa$ B phosphorylation (p-p65 NF- $\kappa$ B), TLR4, and p38 MAPK phosphorylation (p-p38 MAPK). BTLG also reduced miR-21 expression, and the overexpression of the miR-21 inhibitor in H9C2 suppressed apoptosis. Moreover, p-p38 MAPK, TLR4 and p-p65 NF- $\kappa$ B expression were down-regulated in miR-21 inhibitor transfected H9C2s. The inhibition of p38/TLR4/ NF- $\kappa$ B signaling might have occurred via the suppression of miR-21 by BTLG.

**Conclusion:** The results show that BTLG inhibits the inflammatory reaction involved in p38 MAPK/TLR4/ NF- $\kappa$ B signaling pathway and can prevent RA-induced cardiac disease, suggesting that BTLG treatment may be beneficial for the management of arthritic cardiomyopathy.

**Keywords:** Bitongling granules, Arthritic cardiomyopathy, miR-21, NF- $\kappa$ B, Inflammation

This is an Open Access article that uses a funding model which does not charge readers or their institutions for access and distributed under the terms of the Creative Commons Attribution License (<http://creativecommons.org/licenses/by/4.0>) and the Budapest Open Access Initiative (<http://www.budapestopenaccessinitiative.org/read>), which permit unrestricted use, distribution, and reproduction in any medium, provided the original work is properly credited.

Tropical Journal of Pharmaceutical Research is indexed by Science Citation Index (SciSearch), Scopus, International Pharmaceutical Abstract, Chemical Abstracts, Embase, Index Copernicus, EBSCO, African Index Medicus, JournalSeek, Journal Citation Reports/Science Edition, Directory of Open Access Journals (DOAJ), African Journal Online, Bioline International, Open-J-Gate and Pharmacy Abstracts

## INTRODUCTION

Rheumatoid arthritis (RA) is a chronic systemic autoimmune disease the main clinical manifestations and causative factors of which remain unknown. RA is associated with increased cardiovascular morbidity and mortality and a poorly understood pathophysiology [1,]. Clinical and experimental data highlight the diverse mechanisms involved in the development of myocardial dysfunction in RA, including oxidative damage, and cardiac inflammation [2]. Amongst these abnormal conditions, inflammatory responses play an important role during myocardial dysfunction during RA. Chronic inflammation directly and indirectly leads to cardiac tissue damage including necrosis and apoptosis [3]. Understanding the basis for inflammation during RA can contribute to improved disease management.

MicroRNAs (miRNAs) are non-coding ssRNAs of 19-25 nt in length that post-transcriptionally regulate gene expression [4]. Accumulating evidence suggests that miRNAs participate in the regulation of inflammatory processes and reduce the occurrence of inflammation [4]. The expression of miR-21 increases during inflammation in the CD4 + T cells of RA patients, which may be related to an increased risk of RA development [5]. Increased miR-21 expression has also been reported in other inflammatory responses such as allergic airway inflammation [4] and inflammatory bowel disease [6].

Recent studies have revealed the involvement of TLR4/NF- $\kappa$ B signaling with RAs [7]. TLR4-mediated innate immune and inflammatory responses play a key role in RA, primarily through NF- $\kappa$ B signaling [8]. Studies have demonstrated that miR-21 prevents OGD-induced neural stem cell death and apoptotic-associated protein activity through inhibiting JNK and p38 pathways [9].

The apoptosis involving miR-21 in hepatoblastoma cells is also mediated through ASPP2/p38 signaling both *in vitro* and *in vivo* [10], preventing MAPK signaling through targeted inhibition of MAP2K3 [11]. It is therefore considered that miR-21 regulates p38 MAPK and NF- $\kappa$ B signaling and the production of inflammatory cytokines [12]. Bitongling granules are a Traditional Chinese Medicine (TCM) known to improve the clinical symptoms of RA [13]. However, the effectiveness of bitongling granules when treating patients with myocardial inflammation induced by RA requires elucidation.

The aim of this study is to reveal the relationship between bitongling granules, miR-21, p38 MAPK and NF- $\kappa$ B signaling during the downregulation of inflammatory responses in myocardial inflammation induced by RA.

## EXPERIMENTAL

### Animals and BTLG preparation

Twenty adult male Sprague-Dawley (SD) rats weighing 180-220 g were purchased from Western Biotech. Co. Ltd. (Chongqing, China). All animal experiments were performed under protocols approved by the Animal Care and Use Committee (Ethics Committee) of the Anhui University of Chinese medicine (Hefei, China) and also followed international guidelines for animal studies.

BTLG was produced using *Radix aconiti preparata* 3 g, *Radix saposhnikoviae* 10 g, *nidus vespae* 5 g, *Ramulus cinnamomi* 6 g, *Caulis sinomenii* 12 g and *herba ephedrae* 5 g. All were provided by the First Affiliated Hospital of Anhui University of Chinese Medicine. A total of 41 g of crude BTLG was dissolved in 10 ml of physiological saline, topped up to a volume of 20.5 mL in saline and stored at 4 °C.

### Preparation of drug-containing serum

After one week of environmental adaptation, all rats were randomly divided into blank controls (equal volume of 0.9 % saline) and those receiving BTLG suspensions. BTLG was administered once per day (0.7 mL/100 g body weight) through continuous administration via gavage for 3 d. On day 4, rats were administered the full-daily dose for 1 h and anaesthetized with ketamine. Blood samples were collected from the portal vein under aseptic conditions at 37 °C, and samples were centrifuged at 3000 rpm for 10 min at 4 °C. Animal serum in the same group was combined and separated serum was inactivated at 56 °C in a water bath for 30 min. Samples were filtered using a 0.22  $\mu$ m filter and stored at -80 °C prior to preservation.

### Cell culture and treatments

The normal rat myoblast line, H9C2, was obtained from the cell bank of the Chinese academy of sciences (Shanghai, China) and maintained in DMEM/low glucose medium (5.5 mmol/l; Life Technologies, Thermo Fisher Scientific, USA.) containing 10 % fetal bovine serum (FBS; Gibco, Thermo Fisher Scientific, Inc.) and 0.1 % penicillin/streptomycin (Life Technologies, Thermo Fisher Scientific, USA).

Lipopolysaccharides (LPS) was purchased from Sigma-Aldrich (Merck). According to previous studies [14], cells were pretreated with LPS (40 mg/L) for 1 h with blank rat serum at a concentration of 10 % or BTLG drug-containing rat serum at a concentration of 10 % for 48 h.

### Quantitative real-time RT-PCR

Quantitative real-time RT-PCR was performed to assess the transcript levels of miR-21. Total RNA was extracted using TRIzol (Invitrogen), and RNA concentration and integrity were determined. First-strand cDNA synthesis was performed and miR-21 was amplified using the CFX96 real-time PCR system (Bio-Rad, USA). The Real Time SYBR master mix kits were set as follows: 50 °C, 2 min, 95 °C, 10 min; 95 °C, 15 s and 60 °C, 1 min (40 cycles). Fold changes in miR-21 PCR products were calculated after adjusting for GAPDH using the comparative  $-\Delta\Delta$  Ct method. Primers were obtained from Western Biotechnology Corp (Chongqing, China). The primer sequences used are shown in Table 1.

### Cell transfection

siRNA transfections were performed in H9C2 cells cultured in 35 mm culture dishes for 1 day, followed by transfection with the miR-21 inhibitor (5'-UCAACAUCAGUCUGAUAAGCUA-3'; GenePharm, shanghai, China) or non-targeting NC-inhibitor (5'-CAGUACUUUUGUGUAGUA CAA-3'; GenePharm, shanghai, China) using Lipofectamine RNAiMAX (Thermo Fisher Scientific, USA) reagents according to the manufacturer's instructions. After 6 h of transfection, the medium was changed to normal medium supplemented with 10 % FBS. Transfected cells were harvested for proliferation and apoptosis assays, and protein expression was assessed 24 h post-transfection.

### MTT assays and morphological analysis

Cells treated with LPS, or BTLG were incubated with 0.5 mg/mL MTT reagent (Beyotime Biotechnology, China). Cells were then washed and dimethyl sulfoxide (DMSO) was added. Absorbances were measured at 490 nm on a spectrometer (Varioskan LUX, Thermo Fisher, USA). Experiments were replicated three times and the average optical density (OD) values

were obtained. Cell viability rates were calculated as the OD value of the experimental group/the OD value of control group  $\times$  100 %. Morphological analysis was performed on an inverted microscope (Olympus, Tokyo, Japan) at 100 $\times$  magnification.

### Flow cytometry

Apoptotic cells were assessed using Annexin V/7-amino-actinomycin D (AV/7-AAD) staining kits according to the manufacturer's instructions (Beyotime Biotechnology, China). H9C2 cells (1 $\times$ 10<sup>6</sup> per sample) were stained in 500  $\mu$ l binding buffer containing 5  $\mu$ l 7-AAD and 5 $\mu$ l AnnexinV-FITC for 10-15 mins. Binding of Annexin V and 7-AAD were analyzed on a BD FACS Calibur flow cytometer (BD Biosciences, San Jose, USA). The percentage of apoptotic cells (AnnexinV + 7-AAD+) were analyzed across experimental groups.

### Enzyme linked immunosorbent assay (ELISA)

Cytokine concentrations were determined by ELISA according to the manufacturer's protocols (Liankebioscience, Hangzhou, China). Firstly, protein standards and supernatants were added to 96-well ELISA plates and incubated at 37 °C for 1.5 h. ELISA plates were then washed 4-5 times and antibodies (100  $\mu$ L) were added to each well at 37 °C for 1 h. The supernatants of the samples were discarded and plates were labeled with HRP-conjugated secondary antibodies (100  $\mu$ L) at 37 °C in a humidified incubator for 30 min. TMB substrate (100  $\mu$ L) was added to each well and plates were incubated in the dark for 15 min. Stop solution (100  $\mu$ L) was added to each well and OD values were read at 450 nm. Standard curves were obtained using two-fold dilutions for each individual experiment. Samples were assessed in triplicate.

### Western blot analysis

Cells were lysed in RIPA lysis buffer (Beyotime Biotechnology, China) and protein content assessed via BCA assays (Beyotime Biotechnology, China). Proteins (50  $\mu$ g) were resolved on 10 % (w/v) sodium dodecyl sulfate bis-tris gels and transferred to polyvinylidene fluoride (PVDF) membranes.

**Table 1:** Primer sequences used for PCR

Item	Forward	Reverse
	5'CGGTAGCTTATCAGACTG3'	5'GAGCAGGCTGGAGAA3'
GAPDH	5'CCCATCTATGAGGGTTACGC3'	5'TTTAATGTCACGCACGATTC3'

Membranes were blocked in PBST containing 5 % (w/v) skimmed milk powder for 2 h and probed with primary antibodies (TLR4, 1:500; p-p38 MAPK, 1:1000; p38 MAPK, 1:1000; p-p65 NF- $\kappa$ B, 1:1000; p65 NF- $\kappa$ B, 1:1000; GAPDH, 1:2000) (Santa Cruz Biotechnology, CA, USA) overnight at 4 °C. Membranes were washed four times in PBST and incubated with HRP-anti-rabbit or anti-mouse secondary antibodies (1:5000; Proteintech, China) for 1 h. Protein bands were imaged using ECL western blotting substrate Kits (Thermo Scientific/Pierce, USA). Data were analyzed using Quantity One (Bio-Rad, USA) software. GAPDH was used as an internal reference.

### Immunofluorescence staining

Treated H9C2 cells cultured on poly L-lysine (0.1 mg/mL) coated coverslips were fixed in 4 % paraformaldehyde (PFA) and permeabilized with 0.1 % Triton X-100 for 20 min. Cells were blocked in PBS containing 2 % bovine serum albumin (BSA; Sigma-Aldrich) for 1 h and probed at 4 °C with anti-rat TLR4 (1:200, Abcam), anti-rat p-p38 MAPK (1:100, Abcam, USA), and anti-rat p-p65 NF $\kappa$ B antibodies (1:200, Abcam) overnight.

Cells were then washed in PBS and stained with PE-labelled goat anti-rabbit IgG (1:200, Proteintech, China) for 2 h. Cell nuclei were DAPI stained for 5 min at 37 °C and imaged on a high speed and sensitive laser scanning microscope FV3000 (Olympus, Tokyo, Japan) at 200 $\times$  magnification.

### Statistical analysis

Data analysis was performed using GraphPad Prism Version 8.0 (GraphPad Software, La Jolla, CA, USA). Data were expressed as the mean  $\pm$  standard error (SE). All experiments were replicated three times. Data were analyzed using a one-way analysis of variance (ANOVA) followed by Student's t-test.  $P < 0.05$  was considered statistically significant.

## RESULTS

### Expression of miR-21

To investigate the correlation between BTLG and miR-21, qRT-PCRs were performed (Figure 1). Compared to the control group, the expression of miRNA-21 significantly increased in the LPS-treated group, while miR-21 expression significantly declined in the BTLG group compared to the LPS group.

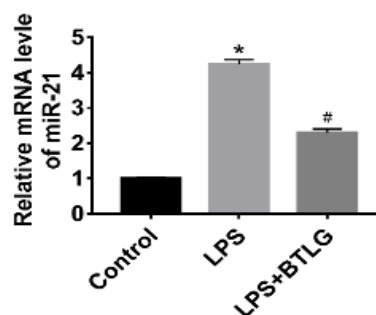


**Figure 1:** MiR-21 expression in H9C2 cells induced by LPS. qRT-PCR was used to analyze the expression of miR-21 in control, lipopolysaccharide (LPS, 40 mg/L), and bitongling granules drug-containing serum (BTLG, 10%) groups. Cells were pretreated with LPS for 1 h or BTLG for 48 h. Data are the mean  $\pm$  SE of three independent experiments;  $n = 6$ , \* $p < 0.05$  vs control, # $p < 0.05$  vs LPS

### Morphological changes in H9C2 cells treated with BTLG

To investigate the effect of BTLG on H9C2 morphology, cells were imaged on an inverted microscope. BTLG treated H9C2 cells grew normally with comparable cell morphologies. In the LPS treatment group, H9C2 cells were small in size, had large refractive indexes and decreased cell densities. Cells treated with the miR-21 inhibitor had a dense, regular arrangement (Figure 2).

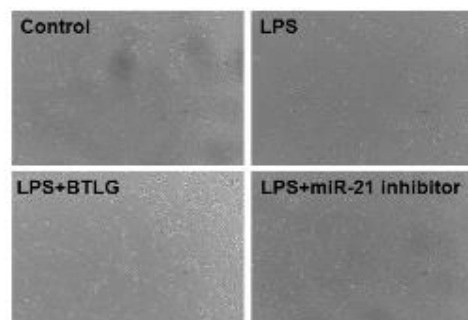


**Figure 2:** Effects of BTLG and miR-21 inhibitors on the morphological changes of H9C2 cells following LPS stimulation. Cells were pretreated with LPS (40 mg/L) for 1 h or BTLG for 48 h. Approximately 12 h post-transfection, miR-21 inhibitor cells were treated with LPS. Untreated cells served as the control group

### BTLG enhances cell viability

To investigate the effect of BTLG on the viability of H9C2 cells, MTT assay was performed. The proliferation rates of each group were comparable at 24 h. However, compared to the LPS group, BTLG and miR-21 inhibitor groups showed increased cell viability at 48 and 72 h

(Figure 3). Compared to BTLG and miR-21 inhibitor groups at 48 and 72 h, no significant differences were observed.

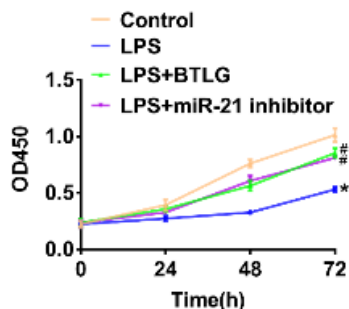


**Figure 3:** Effects of BTLG and miR-21 inhibitors on the viability of cells stimulated with LPS for 24, 48 or 72 h. Data are the means  $\pm$  SEM of three independent experiments;  $n = 10$ , \* $p < 0.05$  vs control, # $p < 0.05$  vs LPS

**BTLG ameliorates LPS-induced apoptosis of H9C2 cells**

To investigate the effect of BTLG on H9C2 apoptosis, Annexin V/7-AAD staining was performed. As shown in Figure 4, apoptotic rates (early and late apoptosis) increased in the LPS groups compared to the control group. However, compared to the LPS group, BTLG and miR-21 inhibitor groups decreased. No differences in the rates of apoptotic cells between BTLG and miR-21 inhibitor groups were observed.

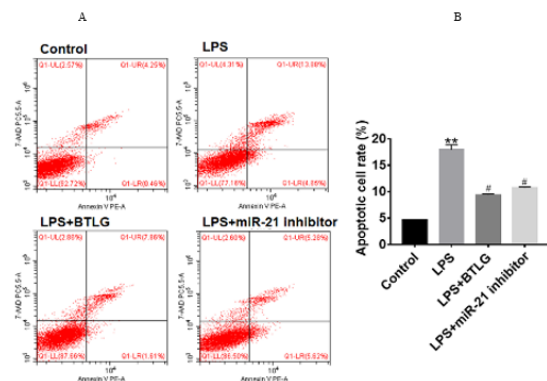


**Figure 4:** Analysis of the effects of BTLG and miR-21 inhibition on apoptosis following LPS stimulation for 24 h in H9C2 cells. (A) Apoptosis was measured by flow cytometry. (B) Percentage of apoptotic H9C2 cells (Q1-UR and Q1-LR) post-treatment. Data are the mean  $\pm$  SE of three independent experiments;  $n = 4$ , \*\* $p < 0.01$  vs control, # $p < 0.05$  vs LPS

**Effect of BTLG on proinflammatory cytokines**

TNF- $\alpha$ , IL-6 and IL-17 are well-characterized proinflammatory markers due to their increased

expression in a number of inflammatory disease states, including RA. To evaluate the effects of BTLG on LPS-induced inflammatory responses, we assessed the production of proinflammatory cytokines by ELISA. Figure 5 A - C shows a significant increase in TNF- $\alpha$ , IL-6 and IL-17 levels after LPS treatment compared to control group. Importantly, BTLG and miR-21 inhibition significantly reduced TNF- $\alpha$ , IL-6 and IL-17 levels.

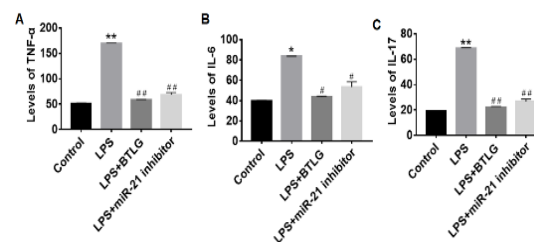


**Figure 5:** Levels of proinflammatory cytokines were evaluated by ELISA. H9C2 cells were treated with LPS (40 mg/L) or LPS (40 mg/L) plus BTLG or miR-21 inhibitor for 48 h. Statistical analysis of (A) TNF- $\alpha$ , (B) IL-6, (C) IL-17 levels;  $n = 6$ , \* $p < 0.05$ , \*\* $p < 0.01$  vs control, # $p < 0.05$ , ## $p < 0.01$  vs LPS

**Effect of BTLG on LPS-induced p38/TLR4/NF- $\kappa$ B signaling**

TLR4 plays a key role in the development and progression of inflammatory responses and adaptive immunity [15]. Compared to the control group (Figure 6A-6B, and 8), LPS stimulation significantly upregulated TLR4 and p-p65 levels as determined by western blot and immunofluorescence. In contrast, BTLG treatment effectively inhibited TLR4 and p-p65 expression, while the miR-21 inhibitor reduced the expression of TLR4 and p-p65 compared to the LPS group.

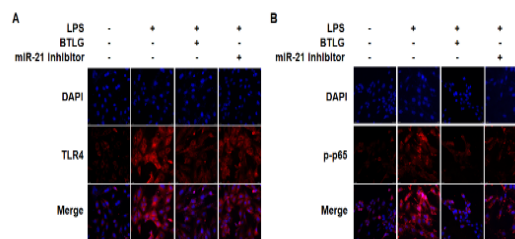


**Figure 6:** Effects of BTLG and miR-21 inhibition on LPS-induced TLR4/ NF- $\kappa$ B signaling in H9C2. Levels of TLR4 (A), and p-p65 (B) were measured by immunofluorescent analysis

p38 is closely related to the inflammatory responses induced by LPS [16] and mediates NF- $\kappa$ B signaling. As shown in Figure 7 and 8, LPS stimulation enhanced the phosphorylation of

p38 compared to the control group. However, BTLG and miR-21 inhibitor treatments decreased the expression of p-p38 MAPK. Taken together, these data suggest that BTLG inhibits the LPS-induced Mactivation of miR-21/p38 /TLR4/NF- $\kappa$ B pathways in H9C2 cells *in vitro*.

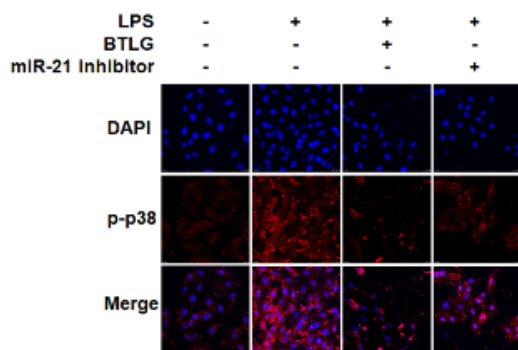


**Figure 7:** Effects of BTLG and miR-21 inhibition on LPS-induced p-p38 signaling in H9C2. Levels of p-p38 were measured by immunofluorescent analysis

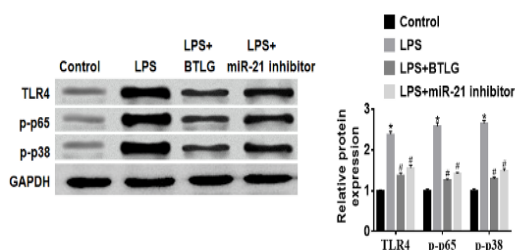


**Figure 8:** Western blot analysis of TLR4, p-p65 and p-p38. After treatment with BTLG for 48 h in LPS-induced inflammatory cells, the expression of TLR4, p-p65, p-p38 were assessed. \* $p < 0.05$  vs control, # $p < 0.05$  vs LPS. Quantification of the relative expression levels. Data are mean  $\pm$  SEM of three independent experiments

## DISCUSSION

Patients suffering from rheumatoid arthritis (RA) face an increased risk of cardiovascular disease (CVD), including myocardial infarction (MI) [17]. Emerging evidence suggests that the increased risk is associated with an overall burden of RA inflammatory disease [18]. In this study, we focused on the effect of BTLG on myocardial inflammation induced by LPS *in vitro*. Moreover, the associated mechanisms for the protective effect of BTLG were investigated.

MiR-21 plays an important role in RA [5] and participates in the development of a variety of inflammatory diseases. In this study, the expression of miR-21 in cardiomyocyte inflammation models induced by LPS was initially

investigated *in vitro*. As expected, a significant increase in miR-21 expression was observed in the LPS group compared to control. miRNA-21 levels in BTLG or other drug treatment groups were significantly lower than the LPS group. The increase in miR-21 may be a result of decreased cardiomyocyte inflammation in RA. However, Toldo and colleagues reported that miR-21 has an indispensable role in mediating cardioprotection in response to H<sub>2</sub>S [4]. Whether these differences are due to different sampling and testing methods, or the progression and stage of the disease requires clarification in future studies.

Toll-like receptors (TLRs) belong to a class of transmembrane pattern-recognition receptors that play crucial roles in the regulation of immune and inflammatory responses [7]. TLR4 is a pattern recognition receptor expressed in a variety of cells that regulates inflammatory stimuli. The MYD88 signaling intermediate is a downstream transduction pathway of TLR4 [5], which leads to the activation of NF- $\kappa$ B and the upregulation of IL-6, TNF- $\alpha$  and IL17. The p38 MAPK subfamily is closely related to LPS induced inflammatory response [16]. NF- $\kappa$ B and p38 MAPK signaling play a key role in inflammatory and stress responses, in addition to cell proliferation and apoptosis [8]. In this study, we investigated the role of BTLG and p38 MAPK/TLR4/NF- $\kappa$ B signaling in cell proliferation, apoptosis and the production of pro-inflammatory cytokines of H9C2 cells.

The results of this study demonstrate that BTLG can reverse the inhibition of proliferation, apoptosis and reduce pro-inflammatory cytokine production by inhibiting p38 MAPK/TLR4/NF- $\kappa$ B signaling. Similar effects were observed for miR-21 inhibition. The levels of p-p38 MAPK, TLR4 and p-p65 NF- $\kappa$ B increased in response to LPS, which was consistent with previous findings. The secretion of IL-17, IL-6 and TNF- $\alpha$  also increased following LPS induction. Upon comparison to the BTLG and miR-21 inhibitor groups, BTLG showed more effective inhibition than the miR-21 inhibitor. Other mechanisms may regulate these pathways which warrants investigation in future studies.

## CONCLUSION

The results demonstrate that BTLG increases H9C2 cell proliferation and apoptosis, but inhibits pro-inflammatory cytokine production through the inhibition of miR-21/p38 MAPK/TLR4/NF- $\kappa$ B signaling, thereby suppressing RA-induced cardiac disease. Therefore, BTLG is a potential therapeutic agent for the management of RA-

induced cardiac disease. Future studies should focus on the mechanisms by which BTLG regulates miR-21 expression. The results presented in this study contribute to our knowledge of the mechanisms involved in the cardioprotection of BTLG.

## DECLARATIONS

### Acknowledgement

This study was supported by Anhui Outstanding Young Talents Support Program (Grant nn.gxyq2018028), Anhui Natural Science Foundation Project (General program) (Grant no. 1808085MH303), The mechanism of xinfeng capsule inhibiting the release of platelet particles based on the PI3K/AKT signaling pathway in AA rats (General program) (Grant no. 81473672), National Natural Science Foundation Youth Fund (Grant no. 81503558), Based on the regulation of programmed death ligand-1 on regulatory T cells to explore the mechanism of lung and intestine combined therapy in the treatment of Sjogren's syndrome (General program) (Grant no. 81774274), The central government guided local science and technology development projects in 2016 (Grant no. [2016]-1188).

### Conflict of Interest

No conflict of interest associated with this work.

### Contribution of Authors

The authors declare that this work was done by the authors named in this article and all liabilities pertaining to claims relating to the content of this article will be borne by them.

### Open Access

This is an Open Access article that uses a funding model which does not charge readers or their institutions for access and distributed under the terms of the Creative Commons Attribution License (<http://creativecommons.org/licenses/by/4.0>) and the Budapest Open Access Initiative (<http://www.budapestopenaccessinitiative.org/read>), which permit unrestricted use, distribution, and reproduction in any medium, provided the original work is properly credited.

## REFERENCES

1. Aviña-Zubieta JA, Choi HK, Sadatsafavi M, Etminan M, Esdaile JM, Lacaille D. Risk of cardiovascular mortality

- in patients with rheumatoid arthritis: A meta-analysis of observational studies. *Arthritis & Rheumatism* 2008; 59(12): 1690-1697.
2. Giles JT, Malayeri AA, Fernandes V, Post W, Blumenthal RS, Bluemke D, Vogel-Claussen J, Szklo M, Petri M, Gelber AC, et al. Left ventricular structure and function in patients with rheumatoid arthritis, as assessed by cardiac magnetic resonance imaging. *Arthritis & Rheumatism* 2010; 62(4): 940-951.
3. Avouac J, Meune C, Chenevier-Gobeaux C, Dieude P, Borderie D, Lefevre G, Kahan A, Allanore Y. Inflammation and disease activity are associated with high circulating cardiac markers in rheumatoid arthritis independently of traditional cardiovascular risk factors. *J Rheumatol* 2014; 41(2): 248-255.
4. Lu TX, Munitz A, Rothenberg ME. MicroRNA-21 is up-regulated in allergic airway inflammation and regulates IL-12p35 expression. *J Immunol* 2009; 182(8): 4994-5002.
5. Dong L, Wang X, Tan J, Li H, Qian W, Chen J, Chen Q, Wang J, Xu W, Tao C, et al. Decreased expression of microRNA-21 correlates with the imbalance of Th17 and Treg cells in patients with rheumatoid arthritis. *J Cell Mol Med* 2014; 18(11): 2213-2224.
6. Ludwig K, Fassan M, Mescoli C, Pizzi M, Balistreri M, Albertoni L, Pucciarelli S, Scarpa M, Sturniolo GC, Angriman I, et al. PDCD4/miR-21 dysregulation in inflammatory bowel disease-associated carcinogenesis. *Virchows Archiv: an international journal of pathology* 2013; 462(1): 57-63.
7. Serasanambati M, Chilakapati SR. Function of Nuclear Factor Kappa B (NF- $\kappa$ B) in Human Diseases-A Review. *South Indian J Biol Sci* 2016; 2(4).
8. Yan S, Wang P, Wang J, Yang J, Lu H, Jin C, Cheng M, Xu D. Long Non-coding RNA HIX003209 Promotes Inflammation by Sponging miR-6089 via TLR4/NF- $\kappa$ B Signaling Pathway in Rheumatoid Arthritis. *Front Immunol* 2019; 10: 2218.
9. Chen R, Tai Y, Zhang Y, Wang L, Yang Y, Yang N, Ma S, Xue F, Wang J. MicroRNA-21 attenuates oxygen and glucose deprivation induced apoptotic death in human neural stem cells with inhibition of JNK and p38 MAPK signaling. *Neurosci Lett* 2019; 690: 11-16.
10. Liu L, Wang L, Li X, Tian P, Xu H, Li Z, Liu E. Effect of miR-21 on apoptosis in hepatoblastoma cell through activating ASPP2/p38 signaling pathway in vitro and in vivo. *Artif Cells, Nanomed Biotechnol* 2019; 47(1): 3729-3736.
11. Yao X, Wang Y, Zhang D. microRNA-21 Confers Neuroprotection Against Cerebral Ischemia-Reperfusion Injury and Alleviates Blood-Brain Barrier Disruption in Rats via the MAPK Signaling Pathway. *Journal of molecular neuroscience*. MN 2018; 65(1): 43-53.
12. Dong X, Kim YS, Kim EK, Shin WB, Park JS, Kim SJ, Go EA, Park PJ, Kwon SC. Scallop Extracts Inhibited LPS-Induced Inflammation by Suppressing MAPK and NF- $\kappa$ B Activation in RAW264.7 Macrophages. *Adv Exp Med Biol* 2019; 1155: 1069-1081.

13. Qin S, Wang Y. Influences of Bitongling Granule on Collagen-induced Arthritis Rats. *J Hubei University Chinese Med* 2011.
14. Wang X, Zhang Q, Ji W. Effect of Tongbi Decoction Serum on Proliferation of Articular Chondrocytes and MMP-3 and TIMP-1 in Cultured Neonatal Rabbits. *Shanghai J Trad Chinese Med* 2006; 40: 64-65.
15. Yang XW, Li YH, Zhang H, Zhao YF, Ding ZB, Yu JZ, Liu CY, Liu JC, Jiang WJ, Feng QJ, et al. Safflower Yellow regulates microglial polarization and inhibits inflammatory response in LPS-stimulated Bv2 cells. *Int J Immunopathol Pharmacol* 2015; 29(1): 54-64.
16. Camacho-Barquero L, Villegas I, Sanchez-Calvo JM, Talero E, Sanchez-Fidalgo S, Motilva V, Alarcon de la Lastra C. Curcumin, a *Curcuma longa* constituent, acts on MAPK p38 pathway modulating COX-2 and iNOS expression in chronic experimental colitis. *Int Immunopharmacol* 2007; 7(3): 333-342.
17. Lindhardtsen J, Ahlehoff O, Gislason GH, Madsen OR, Olesen JB, Torp-Pedersen C, Hansen PR. The risk of myocardial infarction in rheumatoid arthritis and diabetes mellitus: a Danish nationwide cohort study. *Ann Rheum Dis* 2011; 70(6): 929-934.
18. Goodson NJ, Symmons DP, Scott DG, Bunn D, Lunt M, Silman AJ. Baseline levels of C-reactive protein and prediction of death from cardiovascular disease in patients with inflammatory polyarthritis: a ten-year follow-up study of a primary care-based inception cohort. *Arthritis Rheum* 2005; 52(8): 2293-2299.